
PHASE RESONANCE NONLINEAR MODES OF MECHANICAL SYSTEMS

A PREPRINT

Martin Volvert

Space Structures and Systems Laboratory,
Aerospace and Mechanical Engineering Department,
University of Liège, Belgium
m.volvert@uliege.be

Gaëtan Kerschen

Space Structures and Systems Laboratory,
Aerospace and Mechanical Engineering Department,
University of Liège, Belgium
g.kerschen@uliege.be

October 29, 2020

ABSTRACT

Motivated by the lack of a well-defined theoretical relation between nonlinear normal modes and resonances, the present study proposes a generalization of phase resonance to nonlinear mechanical systems which encompasses fundamental, superharmonic and subharmonic resonances. Based on this generalization, a new definition of a nonlinear mode, termed phase resonance nonlinear modes (PRNMs), is established. The PRNMs are illustrated on one- and two-degree-of-freedom systems featuring a cubic nonlinearity.

Keywords nonlinear dynamics · modal analysis · phase resonance

1 Introduction

Modal analysis has been, and continue to be, the dominant dynamical method used in structural design. The goal of modal analysis is to find the vibration modes, resonance frequencies and damping ratios of the considered system [1]. One key assumption of modal analysis is linearity, which, however, real-world structures violate because they may feature advanced materials, friction and contact [2].

The theory of nonlinear normal modes (NNMs) was developed to generalize the concept of vibration mode to nonlinear systems [3]. There exist two main definitions of a NNM based on either periodic motions or invariant manifolds. In direct analogy to a linear mode, Rosenberg defined a NNM as a synchronous vibration of the undamped, unforced system for which all points reach their extreme values or pass through zero simultaneously [4, 5]. This definition was later generalized to non-necessarily synchronous periodic oscillations of the system to encompass modal interactions [6]. The concept of periodic solution was then extended to dissipative systems through an additional damping term which is large enough to compensate for the nonconservative forces [7]. Based on the theory of invariant manifolds, Shaw and Pierre proposed an elegant generalization of a nonlinear mode to damped systems [8, 9]. The manifold defining the NNM is invariant under the flow, i.e., the orbits that start out in the manifold remain in it for all times, which extends the invariance property of linear normal modes to nonlinear systems. Recently, Haller provided exact mathematical existence and uniqueness conditions for NNMs defined as invariant manifolds [10].

The paradigm considered so far in the nonlinear dynamics community assumes that the resonances of the forced system occur in the neighborhood of NNMs. However, several studies showed that this approach may lead to both theoretical and experimental difficulties. On the one hand, through Melnikov analysis, Haller and co-workers highlighted that backbone curves do not necessarily perturb into forced-damped periodic responses, meaning that not all NNMs contribute to shaping the forced response of nonlinear systems [11]. Similarly, Hill et al. evidenced that only those NNMs which are able to transfer a large amount of energy through the fundamental components of the response strongly relate to the forced dynamics [12]. On the other hand, Peeters et al. demonstrated using harmonic balance that multi-point, multi-harmonic forcing is necessary to accurately isolate a conservative NNM, which severely complicates the

experimental realization of NNMs [13]. Other studies also attempted to interpret numerically or experimentally the forced response using backbone curves, see, e.g., [14, 15].

Motivated by the lack of a well-defined theoretical relation between NNMs and resonances, the present study proposes a generalization of *phase resonance* to nonlinear systems. For linear systems, unlike amplitude resonance which occurs at a maximum of the frequency response function, phase resonance takes place when the single-point harmonic forcing and the displacement at the forcing location are in quadrature, i.e., the phase is locked at an angle equal to $\pi/2$. If this linear definition extends to the fundamental resonances of nonlinear systems, as demonstrated in [13] and exploited for experimental modal analysis in [16, 17, 18, 19, 20, 21], we generalize it herein to superharmonic and subharmonic resonances. Specifically, we will show that such resonances may exhibit phase lags that are not necessarily equal to $\pi/2$. Based upon these developments, a new definition of a nonlinear mode, termed phase resonance nonlinear modes (PRNMs), is established. By construction, the PRNMs correspond exactly to the *phase resonance* of a nonlinear system subject to single-point, single-frequency forcing.

The paper is organized as follows. Section 2 considers a single-degree-of-freedom Duffing oscillator under harmonic loading and investigates carefully the phase lag between the displacement and the forcing for fundamental, superharmonic and subharmonic resonances. Section 3 defines the so-called PRNMs and establishes the link with phase resonance. An algorithm for the calculation of PRNMs is also proposed. Section 4 applies the PRNM definition to a two-degree-of-freedom system. Finally, conclusions are drawn in Section 5.

2 Resonances of the Duffing oscillator

The Duffing oscillator comprises a mass attached to linear and cubic springs and a linear damper. The governing equation of motion of the harmonically-forced Duffing oscillator is

$$m\ddot{x}(t) + c\dot{x}(t) + kx(t) + k_{nl}x^3(t) = f \sin \omega t \quad (1)$$

where m , c , k and k_{nl} represent the mass, damping, linear and nonlinear stiffness coefficients, respectively. f is the forcing amplitude whereas ω is the excitation frequency. The natural frequency of the undamped, linearized system is $\omega_0 = \sqrt{\frac{k}{m}}$. The coefficients are set to $m = 1\text{kg}$, $c = 0.01\text{kg/s}$, $k = 1\text{N/m}$ and $k_{nl} = 1\text{N/m}^3$ throughout the present study.

Considering the Fourier decomposition of the displacement

$$x(t) = \frac{c_0}{\sqrt{2}} + \sum_{k=1}^{\infty} \left(s_{\frac{k}{\nu}} \sin \frac{k\omega t}{\nu} + c_{\frac{k}{\nu}} \cos \frac{k\omega t}{\nu} \right) \quad (2)$$

shows that additional resonances exist in this simple system. Specifically, each harmonic component of the displacement can trigger a resonance as long as the relation $\frac{k}{\nu}\omega$ corresponds to the frequency of the fundamental resonance of the system. When the ratio $\frac{k}{\nu}$ is lower (greater) than 1, the resonance is said to be subharmonic (superharmonic) and is located after (before) the fundamental resonance. In the present study, the resonances are divided into four categories, namely

- Fundamental resonance ($k = 1, \nu = 1$);
- Superharmonic resonance $k:\nu$ ($k > \nu, \nu = 1$);
- Subharmonic resonance $k:\nu$ ($\nu > k, k = 1$);
- Other superharmonic and subharmonic resonances $k:\nu$ ($k > 1, \nu > 1$).

Superharmonic and subharmonic resonances can further be divided into subcategories depending on the parity of k and ν .

The goal of this section is to analyze carefully the resonant response of the Duffing oscillator, as previously achieved in [22]. To this end, the system is analyzed considering four different forcing amplitudes f , i.e., 0.01N, 0.25N, 1N and 3N. The nonlinear frequency response curves (NFRCs) computed using the harmonic balance method (HBM) with $8 \times \nu$ subharmonics combined with pseudo arc-length continuation are depicted in Figure 1. For a forcing amplitude of 0.01N in Figure 1a, the only nonlinear effect appearing in the NFRC is the hardening of the fundamental resonance. At 0.25N in Figure 1b, 3:1 superharmonic and 1:3 subharmonic resonance branches appear before and after the fundamental resonance, respectively. It should be noted that the subharmonic resonance is isolated from the main curve. Additional branches corresponding to 2:1, 4:1, 5:1 and 7:1 superharmonic and 1:2 subharmonic resonances

arise in Figure 1c at $1N$. Finally, when the forcing amplitude is $3N$, resonances for which neither k nor ν is equal to one and which are all isolated from the main branch can be observed in Figure 1d. They correspond to $7:3$, $3:2$, $4:3$, $2:3$, $3:4$ and $3:5$ resonances. All those resonances are examined in greater detail hereafter. Particular attention is devoted to the phase difference between the dominant harmonic components of the displacement and the harmonic excitation, computed in the interval $]0; 2\pi[$.

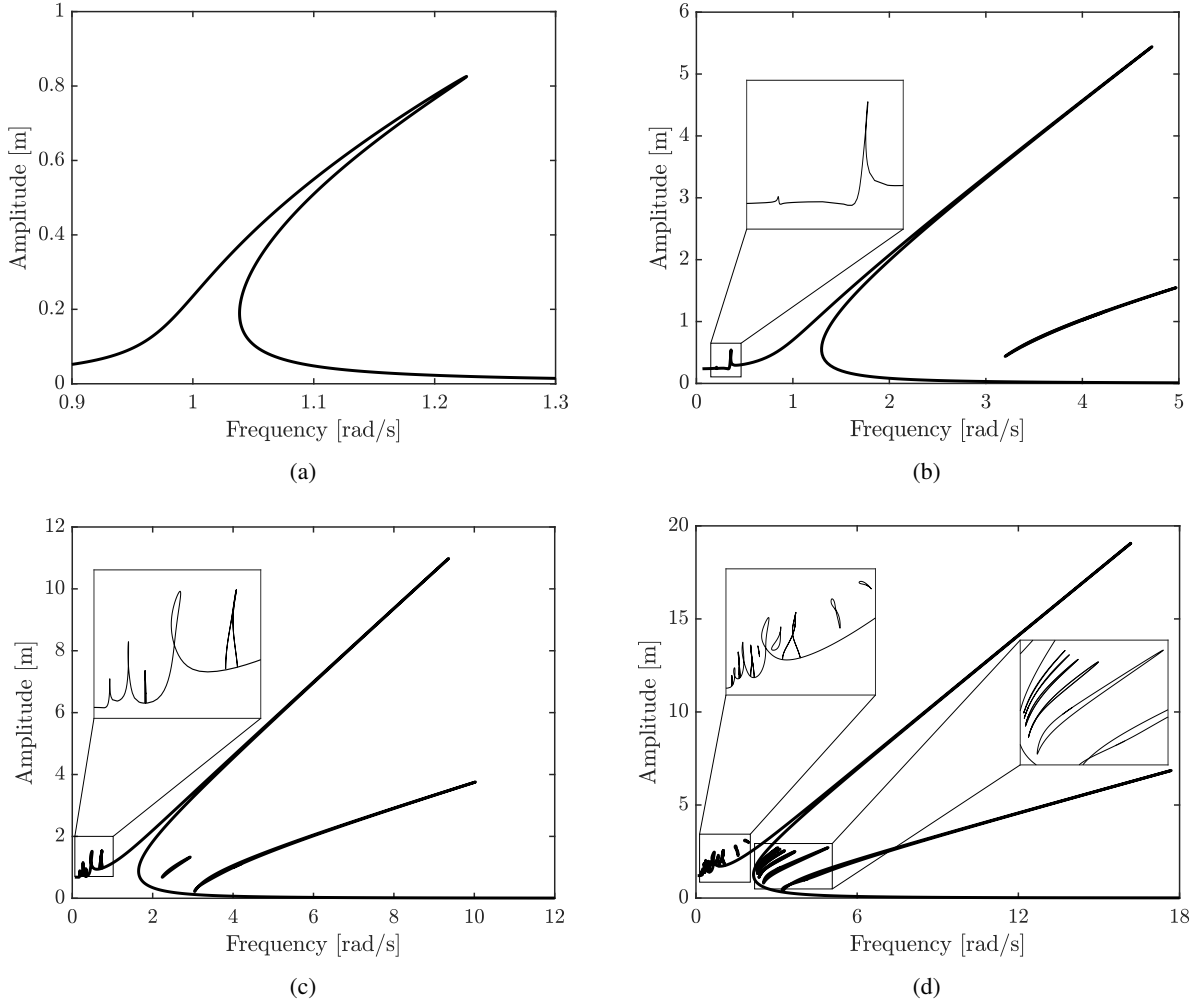


Figure 1: NFRCs of the Duffing oscillator: (a) $f = 0.01N$, (b) $f = 0.25N$, (c) $f = 1N$ and (d) $f = 3N$.

2.1 Fundamental resonance frequency

The amplitude and phase lag of the first harmonic component of the displacement in the neighborhood of the fundamental resonance are displayed in Figures 2a and 2b, respectively. The phase lag varies between 0 and π and passes through $\pi/2$ when nonlinear phase resonance occurs, as discussed in [13]. In view of the light damping, phase resonance is very close to amplitude resonance, which corresponds to the maximum of the NFRC.

2.2 Superharmonic resonances ($k > \nu, \nu = 1$)

In the case of superharmonic resonances, the ratio $\frac{k}{\nu}$ is greater than one and the resonance peaks are located for values of ω lower than ω_0 . A distinction is made between odd and even values of k .

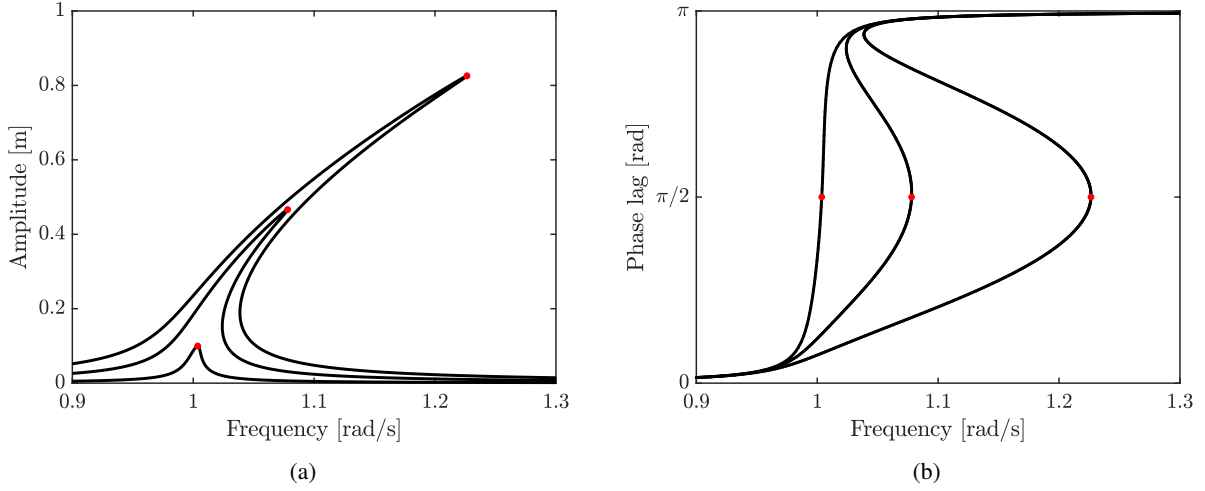


Figure 2: NFRCs of the fundamental resonance of the Duffing oscillator for 3 forcing amplitudes: (a) amplitude and (b) phase lag of the first harmonic component. The red dots correspond to phase resonance [13].

2.2.1 Odd superharmonic resonances

Odd superharmonic resonances are easily calculated, because they appear in the direct continuation of the main branch of the NFRC. Three superharmonic resonances, namely 3:1, 5:1 and 7:1, are represented in Figure 3a. More resonances could have been found if more harmonics were considered in the HBM. The phase lag of the third harmonic component of the 3:1 resonance in Figure 3b is comprised between 0 and π and, as for the fundamental resonance, it passes through $\pi/2$ at resonance. The same observation holds for the other superharmonic resonances. These results suggest that phase quadrature between the forcing and the dominant harmonic component exists at resonance for odd superharmonic branches.

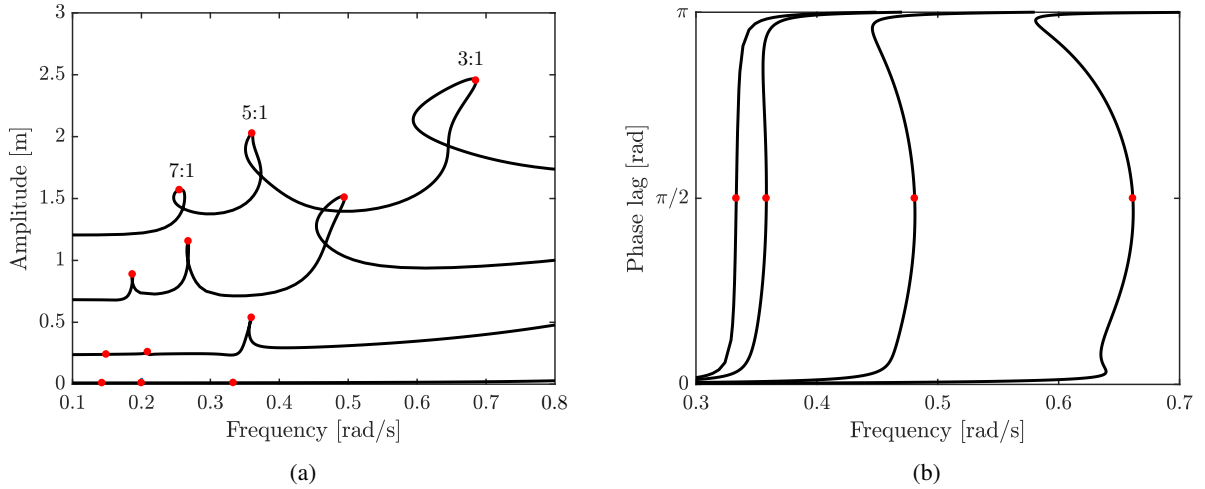


Figure 3: NFRCs of the 3:1, 5:1 and 7:1 superharmonic resonances for 4 forcing amplitudes: (a) amplitude and (b) phase lag of the 3rd harmonic component of the 3:1 resonance (computed with only 3 harmonics for better readability). The points where the phase lag is equal to $\pi/2$ are marked by red dots.

2.2.2 Even superharmonic resonances

Contrary to odd superharmonic resonances, the 2:1, 4:1, 6:1 and 8:1 superharmonic resonances in Figure 4 bifurcate out from the main NFRC. In addition, the phase lag of the second harmonic component of the 2:1 resonance in Figure

4b is comprised between $\pi/2$ and π and passes through $3\pi/4$ at resonance. The same observation holds for the 4:1, 6:1 and 8:1 resonances.

For each resonance, the continuation procedure goes two times through the branch, with a phase shift of π between the two solutions. This phase shift is clearly seen in Figure 4b. The corresponding time series in Figure 5 show that the solutions are not symmetric with respect to the mid period and are opposite of each other with a phase shift of π . They share, however, the same maximum amplitude in absolute value.

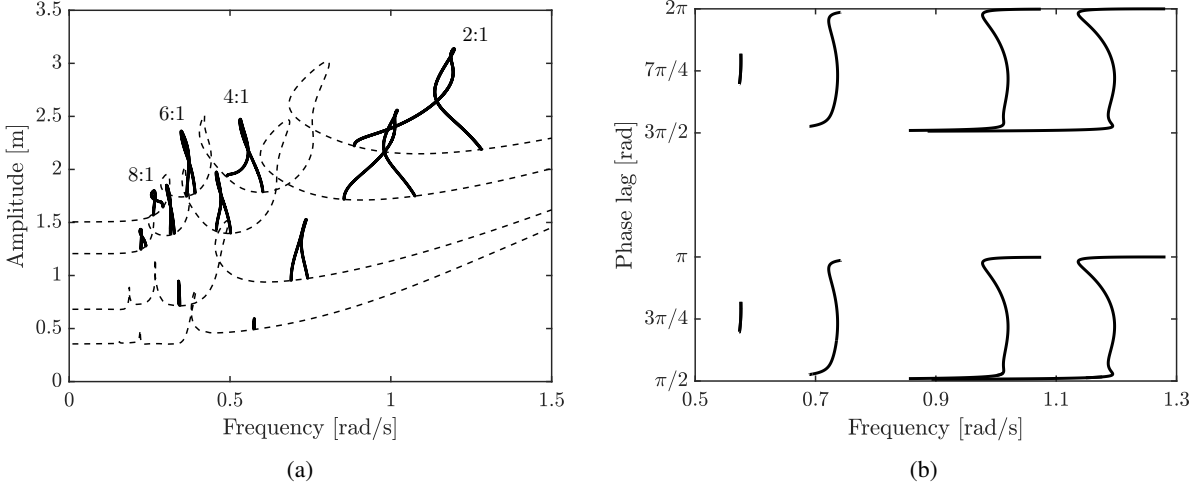


Figure 4: NFRCs of the 2:1, 4:1, 6:1 and 8:1 superharmonic resonances for 4 forcing amplitudes: (a) amplitude and (b) phase lag of the 2nd harmonic component of the 2:1 resonance.

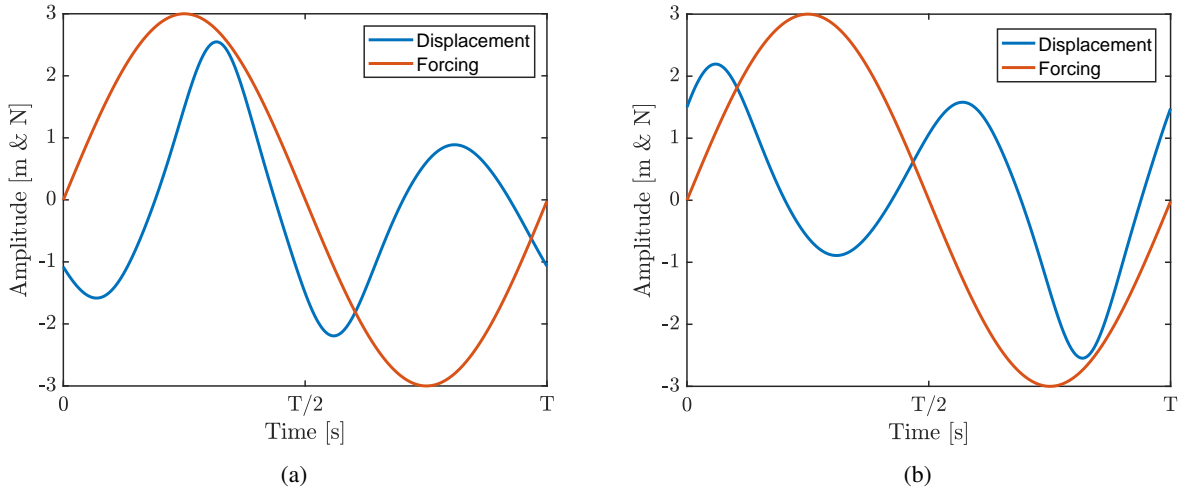


Figure 5: Time series corresponding to two different branches of the 2:1 superharmonic resonance: (a) phase lag = $3\pi/4$ and (b) phase lag = $7\pi/4$.

2.3 Subharmonic resonances ($\nu > k, k = 1$)

The ratio $\frac{k}{\nu}$ is now lower than one, and the resonance branches are located beyond the fundamental resonance. An important feature of subharmonic resonances is that they appear as branches isolated from the main NFRC (see Figure 1); they are thus more challenging to compute.

To obtain a complete periodic response, several cycles of the harmonic forcing have to be considered. This implies that the solution can begin at ν possible times, i.e., each time the forcing starts a new cycle: $0, T, \dots, (\nu - 1)T$.

This is illustrated in Figure 6 for the 1:3 subharmonic resonance. Different initial conditions marked by the red dots can thus trigger the resonance. However, all three solutions are the same but shifted by $2\pi/\nu$, which leads us to conclude that, for each resonance with $\nu > 1$, there exists $\nu - 1$ other equivalent solutions shifted by $2i\pi/\nu$, where $i = 1, \dots, \nu - 1$.

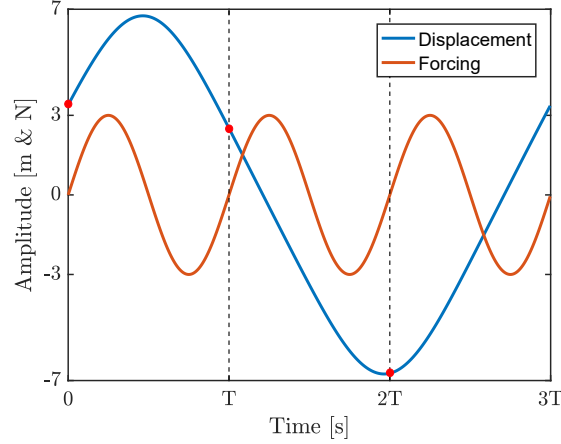


Figure 6: Time series of the 1:3 subharmonic resonance, $f = 3N$ and $\omega = 17.44\text{rad/s}$. The different initial conditions are marked by red dots.

2.3.1 Odd subharmonic resonances

The 1:3 subharmonic resonance observed in Figure 1b is displayed in Figure 7. The corresponding phase lag for the $1/3^{\text{rd}}$ harmonic component is bounded by $\pi/3$ and $2\pi/3$. Since the branch is isolated, the phase lag is twice equal to $\pi/2$, which happens at the extremities of the isolated branch.

For higher-order $1 : \nu$ subharmonic resonances, the phase lag of the $1/\nu^{\text{th}}$ harmonic component is located in the interval $[\pi/2 \pm \pi/2\nu]$.

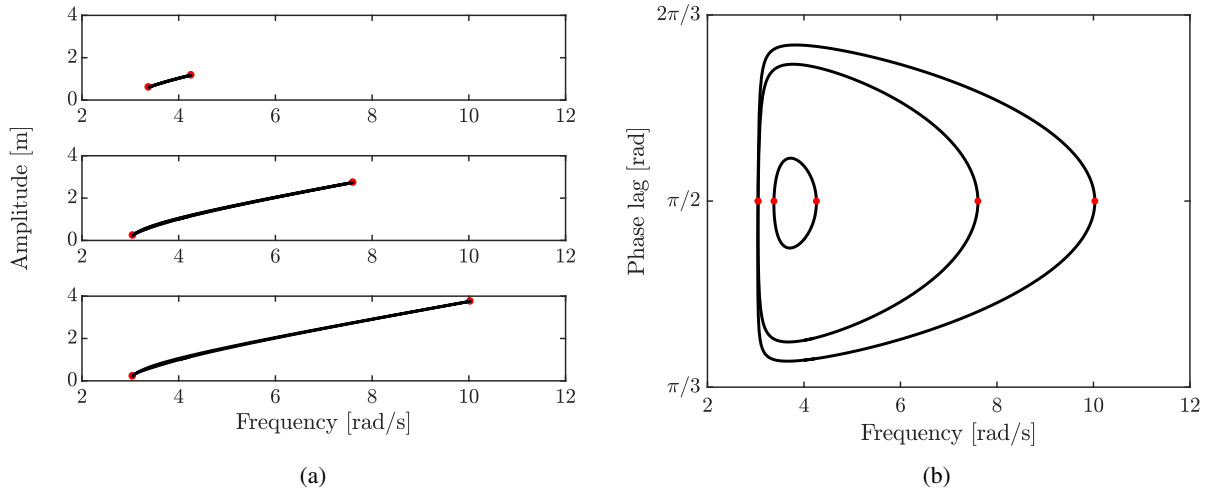


Figure 7: NFRCs of the 1:3 subharmonic resonance for 3 forcing amplitudes: (a) amplitude and (b) phase lag of the $1/3^{\text{rd}}$ harmonic component.

2.3.2 Even subharmonic resonances

As for even superharmonic resonances, the phase lag of even subharmonic resonances is not centered around $\pi/2$. Specifically, for the 1:2 resonance in Figure 8, it is centered around $3\pi/8$ and comprised between $\pi/4$ and $\pi/2$. We

note that a second solution, whose maximum amplitude in absolute value is the same as in Figure 8a and whose phase lag is shifted by π/ν can be found.

For higher-order 1 : ν resonances, the phase lag envelope is $\pi/2\nu$ and centered around $3\pi/4\nu$.

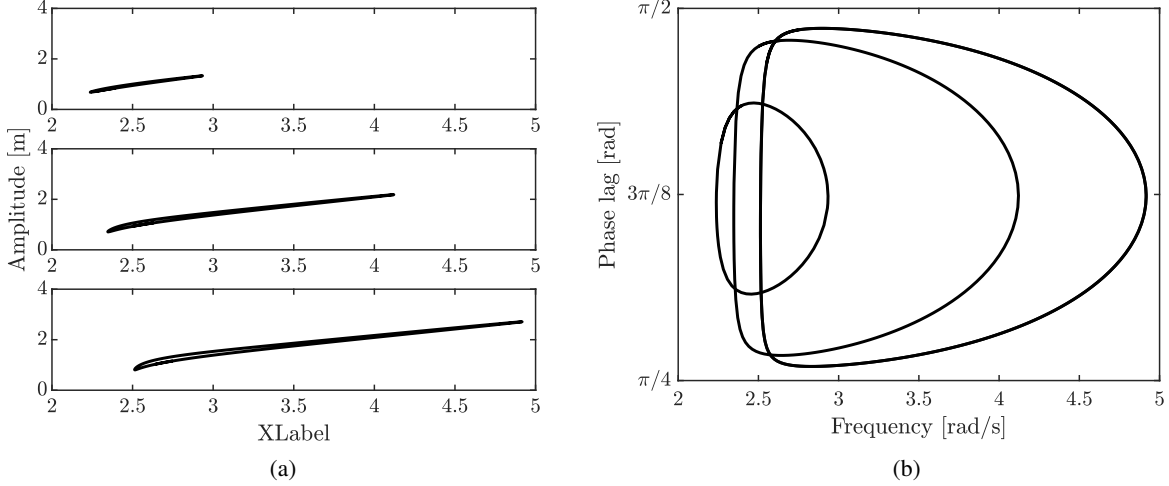


Figure 8: NFRCs of the 1:2 subharmonic resonance for 3 forcing amplitudes: (a) amplitude and (b) phase lag of the 1/2 harmonic component.

2.4 Other superharmonic and subharmonic resonances ($k > 1, \nu > 1$)

The last resonances considered herein are characterized by a ratio k/ν where neither k nor ν is equal to 1. Figure 1d shows that such resonances are all isolated from the main NFRC; basins of attraction are required to find them all. Superharmonic and subharmonic resonances are studied based on the parity of k and ν , i.e., k and ν are odd, k is odd, ν is even and k is even, ν is odd.

2.4.1 k and ν are odd

This type of resonance behaves similarly as odd subharmonic resonances. However, in addition to the solution centered around $\pi/2$, a second solution shifted by $\pm\pi/\nu$ also exists. Unlike even resonances, this second solution is neither the same as the first one nor the opposite. For illustration, Figure 9a and 9b present the amplitude and phase lag of the 7/3 harmonic component for the 7:3 resonance. As the forcing amplitude increases, the two solutions get closer to each other; their phase lag oscillates around $\pi/2$ and $\pi/6$. Eventually, the two solutions merge, as shown in Figure 10.

For the 3:5 resonance in Figures 9c and 9d, the phase lag is also centered around $\pi/2$.

2.4.2 k is odd and ν is even

Two kinds of resonances are studied in Figure 11, namely the 3:2 superharmonic and 3:4 subharmonic resonances. Such resonances follow the same rules as for even subharmonic resonances, i.e., the phase lag of the harmonic k/ν oscillates in the interval $[3\pi/4\nu \pm \pi/4\nu]$. Again, a second solution shifted by π/ν exists and is the opposite of the first one.

2.4.3 k is even and ν is odd

Figure 12 represents the superharmonic 4:3 and the subharmonic 2:3 resonances. The phase lag of the considered harmonic is centered around $3\pi/4\nu$ and the envelope is $\pi/2\nu$. Again, a second solution of same maximum absolute value can be found with a phase lag shifted by π/ν .

2.5 Summary

Table 1 presents a summary of the characteristics of the phase lag of the different resonance branches investigated in the previous sections. It shows that, for varying forcing amplitudes, phase resonance occurs for a well-defined phase

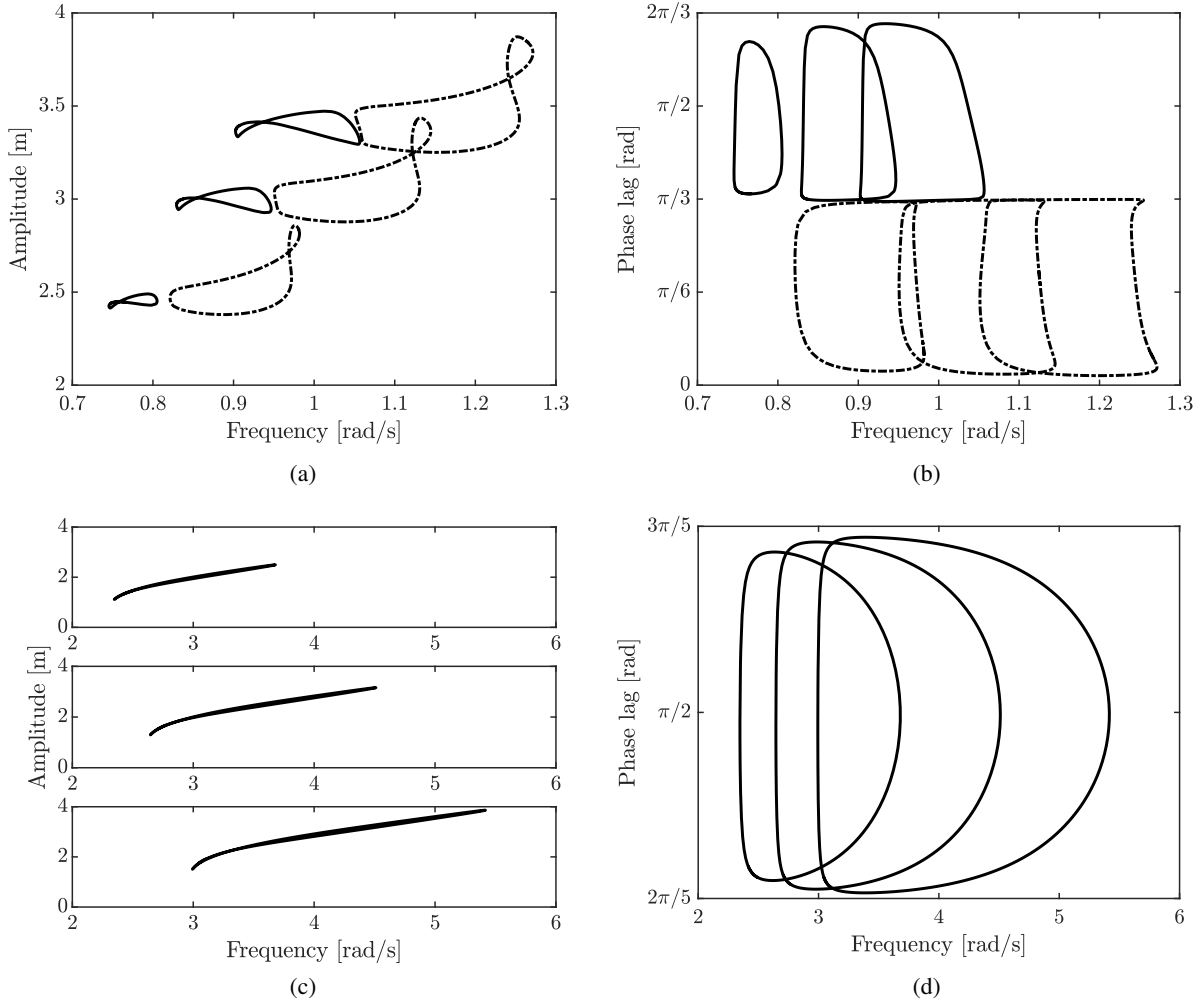


Figure 9: NFRCs of the 7:3 and 3:5 resonances for 3 forcing amplitudes: (a) amplitude - 7:3, (b) phase lag - 7:3, (c) amplitude - 3:5 and (d) phase lag - 3:5.

	k & ν are odd	k or ν is even
Phase lag at resonance	$\pi/2$	$3\pi/4\nu$
Phase lag envelope	π/ν	$\pi/2\nu$

Table 1: Phase lag of the k/ν harmonic component of the $k : \nu$ resonance.

lag between the k/ν harmonic component of the $k : \nu$ resonance and the external forcing. Specifically, it takes place when the phase lag is $\pi/2$ when both k and ν are odd and $3\pi/4\nu$ when either k or ν is even. We recall that other solutions with a phase lag shifted by $\pm\pi/\nu$ may exist, but are not considered in the table.

3 Phase Resonance Nonlinear Modes

For linear systems, phase resonance takes place when the single-point harmonic forcing and the displacement at the forcing location are in quadrature, i.e., the phase is locked at $\pi/2$ [23]. As illustrated in Figure 2 and first demonstrated in [13], this linear definition extends to the fundamental resonances of nonlinear systems.

The results in the previous section allow us to generalize the concept of phase resonance to superharmonic and subharmonic resonances of nonlinear systems. Indeed, they demonstrate that the phase lag can still be used as a robust criterion to track the locus of their resonance peaks, as carried out for fundamental resonances in [17]. The key finding

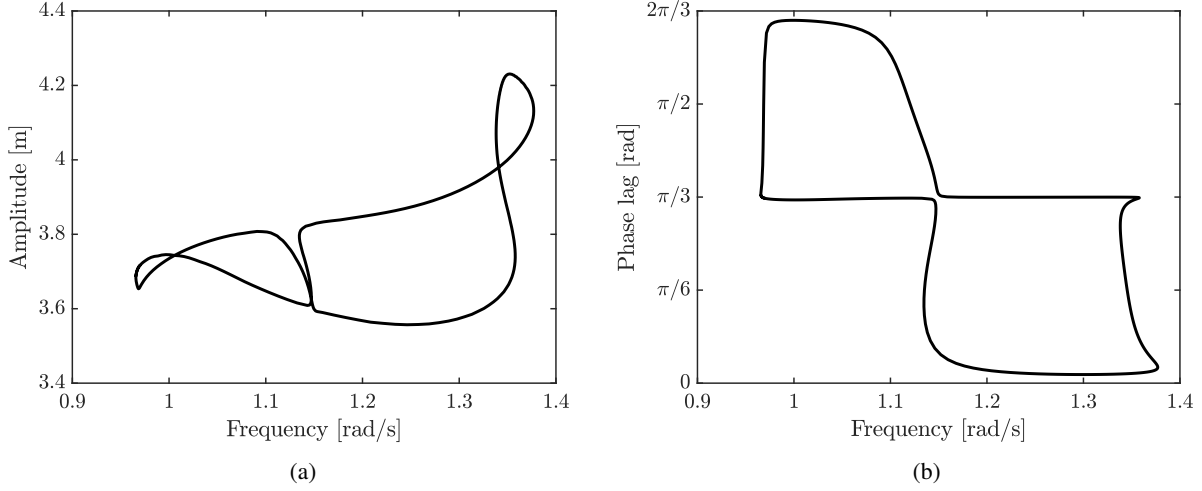


Figure 10: Merging of the 7:3 resonances: (a) amplitude and (b) phase lag of the 7/3 harmonic component.

is that phase quadrature is no longer necessarily achieved for such resonances. Table 1 indicates the conditions which should be considered for the characterization of the different families of superharmonic and subharmonic resonances.

3.1 A new nonlinear normal mode definition

Considering the unforced linear oscillator

$$m\ddot{x}(t) + c\dot{x}(t) + kx(t) = 0, \quad (3)$$

velocity feedback can be considered to drive the system into resonance [7, 24]:

$$m\ddot{x}(t) + c\dot{x}(t) + kx(t) - \mu\dot{x}(t) = 0 \quad (4)$$

where the feedback term $\mu\dot{x}(t)$ plays the role of *virtual forcing*. Because this virtual forcing and the velocity are collinear, phase quadrature with the displacement $x(t)$, and, hence, phase resonance, is naturally enforced when $\mu = c$.

The new NNM definition proposed in this paper, termed phase resonance nonlinear modes (PRNMs), generalizes this strategy to nonlinear systems:

The PRNMs of the $k : \nu$ resonance correspond to the periodic responses obtained by feeding back the T -periodic velocity of the harmonic component k/ν shifted by the delay $\nu\alpha/k\omega$ into the autonomous system.

Mathematically, the following equation is to be solved for the Duffing oscillator:

$$m\ddot{x}(t) + c\dot{x}(t) + kx(t) + k_{nl}x^3(t) - \mu\dot{x}_{\frac{k}{\nu},T}\left(t - \frac{\nu\alpha}{k\omega}\right) = 0, \quad (5)$$

where ω is the frequency at which the PRNMs are to be calculated, and T is the corresponding period. $\alpha = \pi/2 - \delta$ where δ is the phase lag at resonance given in Table 1. For instance, $\alpha = 0$ for all resonances for which k and ν are odd. The ratio $\frac{\nu}{k}$ in the delay accounts for the fact that the period of the fundamental harmonic component is k/ν times that of the k/ν harmonic component.

Considering the 1:2 subharmonic resonance ($k = 1, \nu = 2$) as an illustrative example, Figure 13 shows the three steps to calculate the velocity feedback. The original velocity $\dot{x}(t)$ is represented in Figure 13a whereas the velocity feedback $\dot{x}_{\frac{k}{\nu},T}(t - \frac{\nu\alpha}{k\omega})$ is depicted in Figure 13d. The first step is to filter out all the harmonic components of $\dot{x}(t)$ that are different from k/ν to obtain $\dot{x}_{\frac{k}{\nu}}(t)$ in Figure 13b. This signal is renamed $\dot{x}_{\frac{k}{\nu},\frac{\nu}{k}T}(t)$ to clearly indicate that its period is $\frac{\nu}{k}T$. Second, the remaining velocity signal is transformed into a T -periodic signal $\dot{x}_{\frac{k}{\nu},T}(t)$ in Figure 13c. The third step delays the resulting velocity by the angle $\frac{\nu}{k}\alpha$, i.e., $\pi/4$ for the 1:2 resonance, to calculate $\dot{x}_{\frac{k}{\nu},T}(t - \frac{\nu\alpha}{k\omega})$ in Figure 13d.

For multi-degree-of-freedom systems, the velocity feedback is applied at the degree of freedom where the external forcing is located.

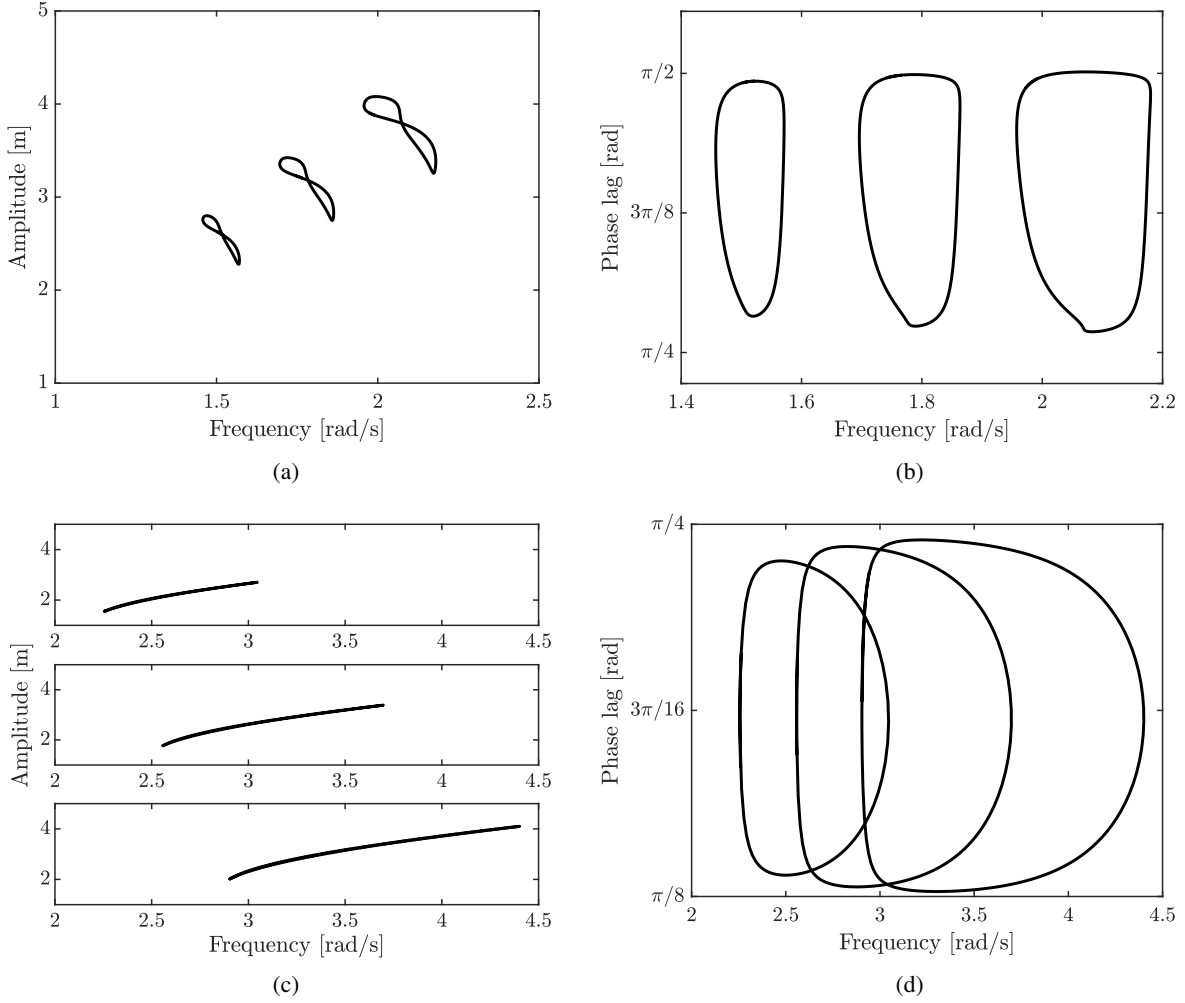


Figure 11: NFRCs of the 3:2 and 3:4 resonances for 3 forcing amplitudes: (a) amplitude - 3:2, (b) phase lag - 3:2, (c) amplitude - 3:4 and (d) phase lag - 3:4.

3.2 Numerical calculation of PRNMs

Although a shooting algorithm could be used, the calculation of the PRNMs lends itself very well to the HBM. Indeed, by definition, HBM separates the response into different harmonic components. Furthermore, no interpolation to render the signal T -periodic is needed.

We consider a n -degree-of-freedom system with harmonic forcing applied at the l -th degree of freedom:

$$\mathbf{M}\ddot{\mathbf{x}}(t) + \mathbf{C}\dot{\mathbf{x}}(t) + \mathbf{K}\mathbf{x}(t) + \mathbf{f}_{nl}(\mathbf{x}(t), \dot{\mathbf{x}}(t)) = \mathbf{f}(t) \quad (6)$$

The displacement and nonlinear force vectors are approximated by truncated Fourier series:

$$\mathbf{x}(t) = \frac{\mathbf{c}_0^x}{\sqrt{2}} + \sum_{k=1}^{N_h} \left(\mathbf{s}_{\frac{k}{\nu}}^x \sin \frac{k\omega t}{\nu} + \mathbf{c}_{\frac{k}{\nu}}^x \cos \frac{k\omega t}{\nu} \right) \quad (7)$$

$$\mathbf{f}_{nl}(t) = \frac{\mathbf{c}_0^f}{\sqrt{2}} + \sum_{k=1}^{N_h} \left(\mathbf{s}_{\frac{k}{\nu}}^f \sin \frac{k\omega t}{\nu} + \mathbf{c}_{\frac{k}{\nu}}^f \cos \frac{k\omega t}{\nu} \right) \quad (8)$$

or, in a more compact form,

$$\mathbf{x}(t) = (\mathbf{Q}(t) \otimes \mathbb{I}_n) \mathbf{X} \quad (9)$$

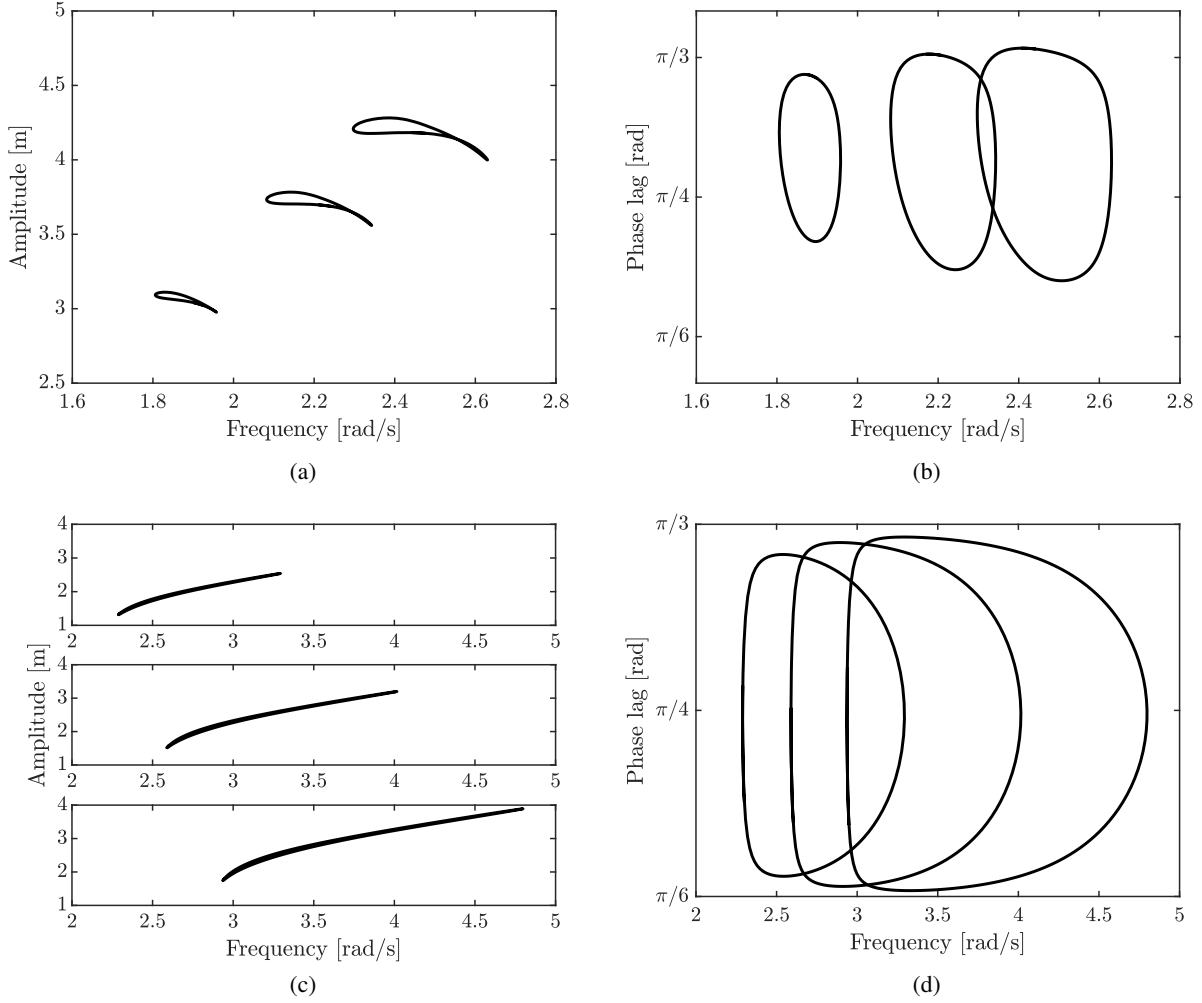


Figure 12: NFRCs of the 4:3 and 2:3 resonances for 3 forcing amplitudes: (a) amplitude - 4:3, (b) phase lag - 4:3, (c) amplitude - 2:3 and (d) phase lag - 2:3

$$\mathbf{f}_{nl}(t) = (\mathbf{Q}(t) \otimes \mathbb{I}_n) \mathbf{F}_{nl} \quad (10)$$

where $\mathbf{Q}(t)$ is a vector containing the sine and cosine terms of the Fourier decomposition, and \mathbf{X} and \mathbf{F}_{nl} are vectors containing the Fourier coefficients of the displacement and nonlinear forces, respectively. By inserting Equations (9) and (10) into the equations of motions (6) and removing the time dependency with a Galerkin procedure, the NFRCs can be obtained by solving the equations of motions in the frequency domain:

$$\mathbf{A}(\omega) \mathbf{X} + \mathbf{F}_{nl}(\mathbf{X}) - \mathbf{F} = 0 \quad (11)$$

where $\mathbf{A}(\omega) = \nabla^2(\omega) \otimes \mathbf{M} + \nabla(\omega) \otimes \mathbf{C} + \mathbb{I}_{2N_h} \otimes \mathbf{K}$ is the dynamic stiffness matrix, and the operator $\nabla(\omega) = \text{diag}(0, \nabla_1, \dots, \nabla_k, \dots, \nabla_{N_h})$ is a differential operator that comes from the time derivative of $\mathbf{Q}(t)$:

$$\nabla_k = k \begin{bmatrix} 0 & -\frac{\omega}{\nu} \\ \frac{\omega}{\nu} & 0 \end{bmatrix} \quad (12)$$

When the forcing frequency ω is specified, Equations (11) provide $2N_h + 1$ equations for $2N_h + 1$ unknowns.

To calculate the PRNMs, we replace the harmonic loading at the l -th degree of freedom with the proposed velocity feedback:

$$\mathbf{A}(\omega) \mathbf{X} + \mathbf{F}_{nl}(\mathbf{X}) - \mu (\mathbf{R}_\alpha \mathbf{T}_T \mathbf{T}_f \nabla(\omega) \otimes \mathbb{I}_l) \mathbf{X} = 0 \quad (13)$$

where

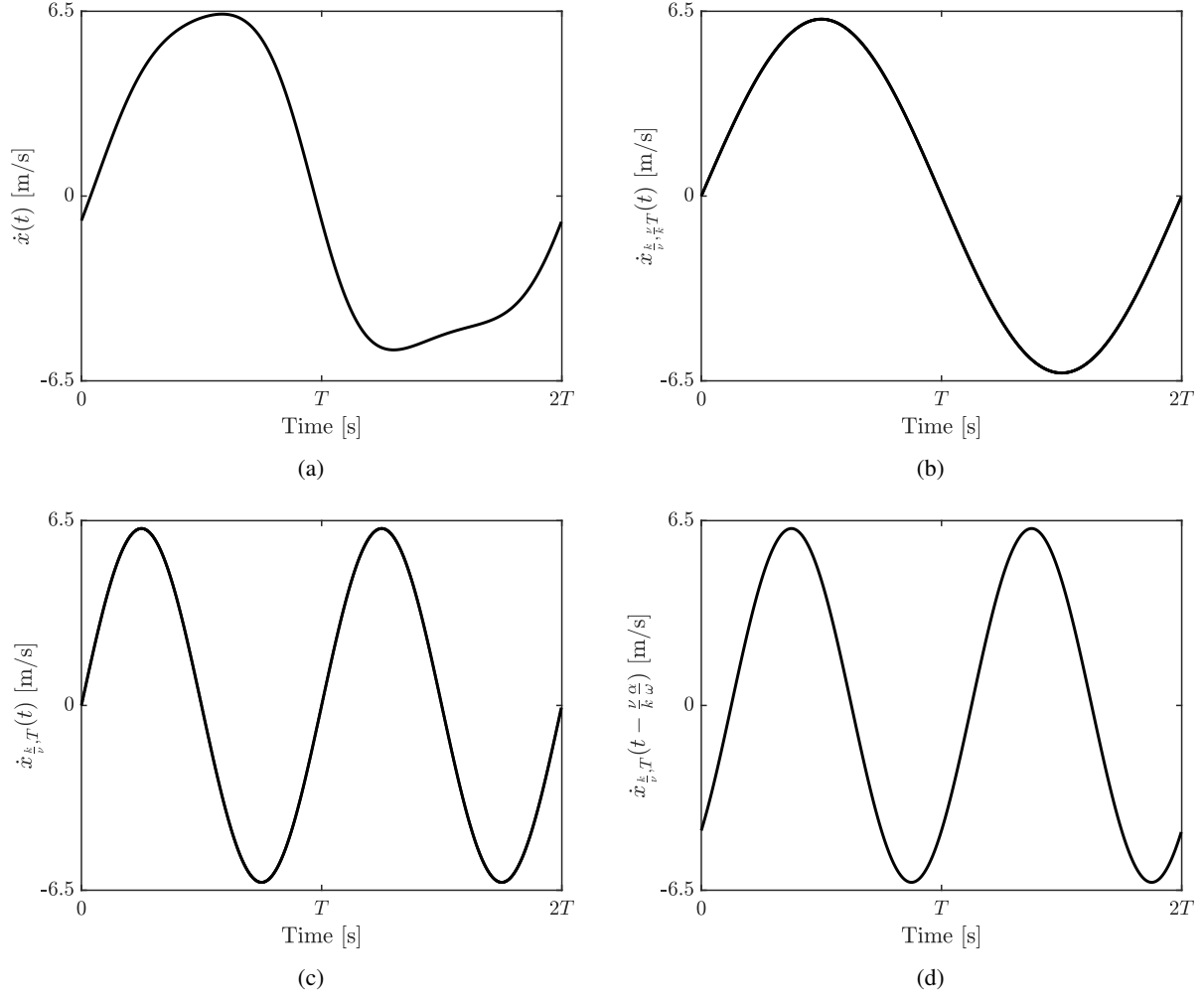


Figure 13: Calculation of the velocity feedback: (a) original velocity, (b) after step 1 (filtering), (c) after step 2 (T -periodic) and (d) after step 3 (delay).

- $(\nabla(\omega) \otimes \mathbb{I}_l) \mathbf{X}$ contains only the Fourier coefficients of the velocity measured at the l -th degree of freedom. \mathbb{I}_l is a $(n \times n)$ a null matrix except for the l -th diagonal term which is equal to 1.
- \mathbf{T}_f is a $(2N_h + 1) \times (2N_h + 1)$ null matrix except for the two diagonal elements corresponding to the k/ν harmonic component which are equal to 1. \mathbf{T}_f thus filters out all the harmonic components different from k/ν , as schematized in the time domain in Figure 13b.
- \mathbf{T}_T is a $(2N_h + 1) \times (2N_h + 1)$ null matrix except for the elements whose rows and columns correspond to the fundamental resonance and k/ν harmonic components, respectively. Those elements are equal to 1. \mathbf{T}_T transforms the velocity into a T -periodic signal, see Figure 13c.
- $\mathbf{R}_\alpha = \text{diag}(0, \mathbf{0}, \dots, \mathbf{R}, \dots, \mathbf{0})$ is a rotation matrix which assigns a phase lag $\nu\alpha/k$ to the fundamental harmonic component of the filtered and T -periodic signal, as in Figure 13d, where

$$\mathbf{R} = \begin{pmatrix} \cos \frac{\nu}{k}\alpha & \sin \frac{\nu}{k}\alpha \\ -\sin \frac{\nu}{k}\alpha & \cos \frac{\nu}{k}\alpha \end{pmatrix}. \quad (14)$$

For fundamental, odd superharmonic and odd subharmonic resonances, $\alpha = 0$, which means that the rotation matrix \mathbf{R} is the identity matrix. For the other resonances, $\alpha = \pi/2 - 3\pi/4\nu$.

Compared to Equation (11), because the gain μ is an additional unknown, Equation (13) comprises $2N_h + 1$ equations for $2N_h + 2$ unknowns. An additional equation is therefore required to close the system. This equation, termed

phase condition, sets the sine coefficient of the k/ν harmonic component to 0. Eventually, by solving equation (13), any resonance can be characterized at different amplitudes by taking the frequency ω as continuation parameter. The PRNMs and the corresponding resonance frequencies are obtained through vector \mathbf{X} and ω , respectively.

To initiate the continuation process, the PRNM algorithm requires an initial guess which is taken as one point on the NFRC located in the vicinity of the resonance of interest. This strategy is easily implemented for resonances that appear in the direct continuation of the main branch of the NFRC, namely for fundamental and $k : 1$ superharmonic resonances. Because the other resonances appear as isolated branches, the computation of basins of attraction is required to provide the initial guess.

3.3 PRNMs of the Duffing oscillator

3.3.1 Fundamental resonance

The PRNM backbone of the fundamental resonance is superposed to the NFRCs of the Duffing oscillator in Figure 14. As anticipated, the backbone goes exactly through the $\pi/2$ phase lag points in Figure 14b and traces very closely the locus of the resonance peaks of the different NFRCs in Figure 14a. Figures 14c and 14d show the evolution of the gain μ with respect to the amplitude and frequency of the forcing, respectively. As expected, when ω is close to ω_0 , *i.e.*, the system behaves almost linearly, μ tends to the value of the damping coefficient $c = 0.01\text{kg/s}$.

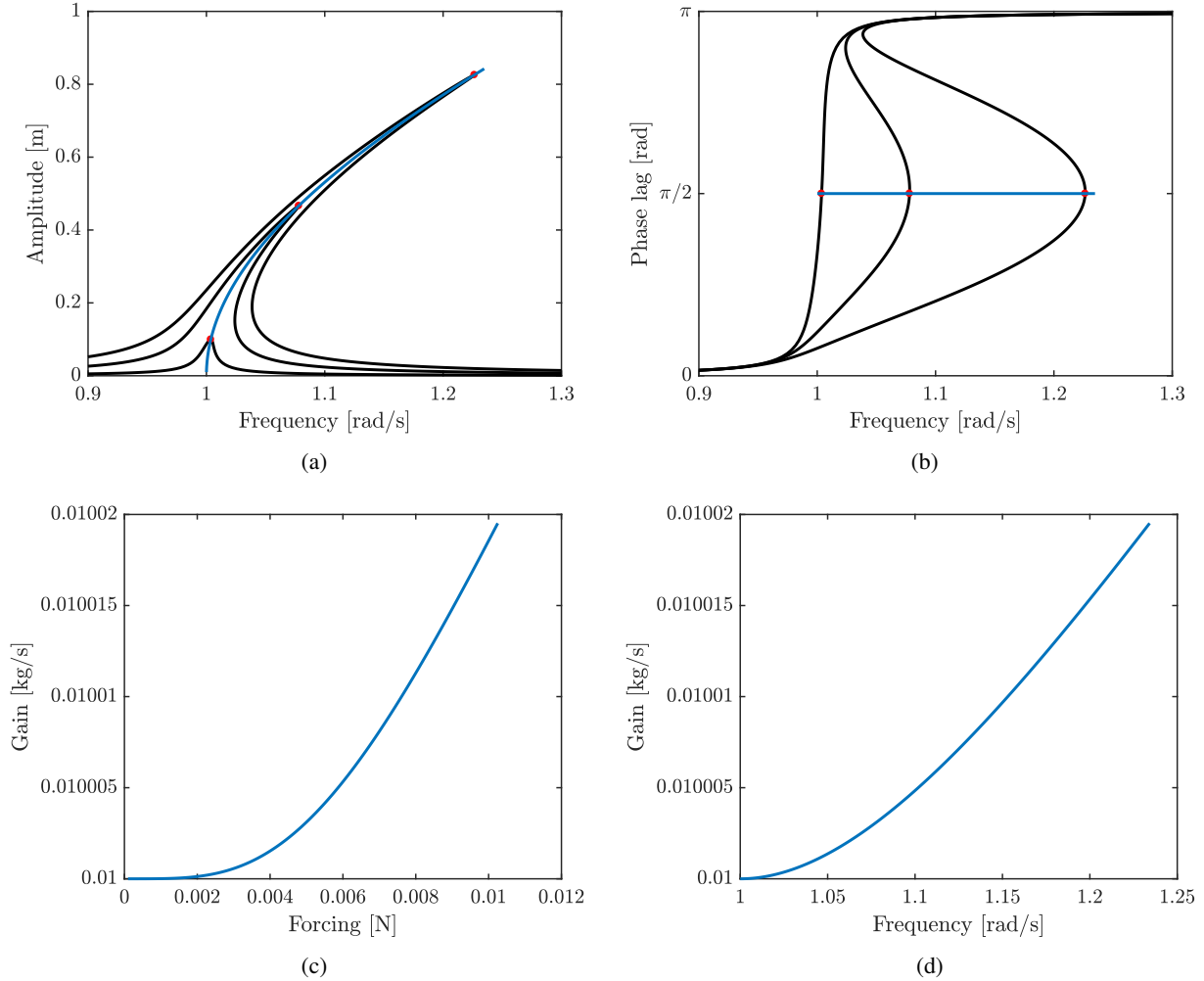


Figure 14: NFRCs and PRNMs of the fundamental resonance of the Duffing oscillator for 3 forcing amplitudes: (a) amplitude, (b) phase lag, (c) gain vs. forcing, (d) gain vs. frequency. Black: NFRC; blue: PRNM.

3.3.2 Superharmonic resonances

For odd and even superharmonic resonances, the phase lags are $\pi/2$ and $3\pi/4$, respectively. The PRNM backbones corresponding to 3:1 and 2:1 resonances are shown in Figures 15 and 16, respectively. These figures confirm the relevance of the PRNMs for the characterization of superharmonic resonances.

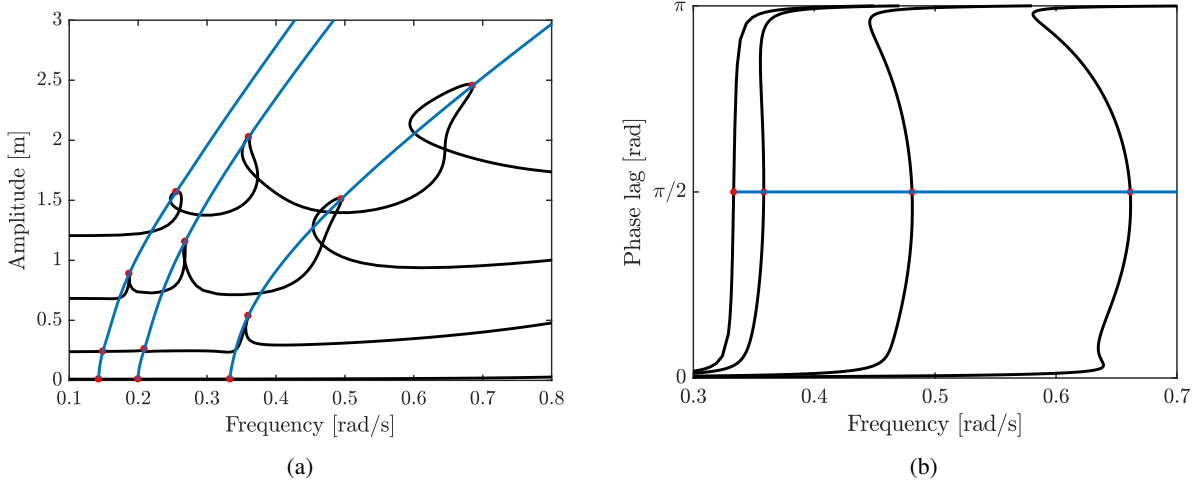


Figure 15: NFRCs and PRNMs of the odd superharmonic resonances for 4 forcing amplitudes: (a) amplitude and (b) phase lag of the 3rd harmonic component of the 3:1 superharmonic resonance. Black: NFRC; blue: PRNM.

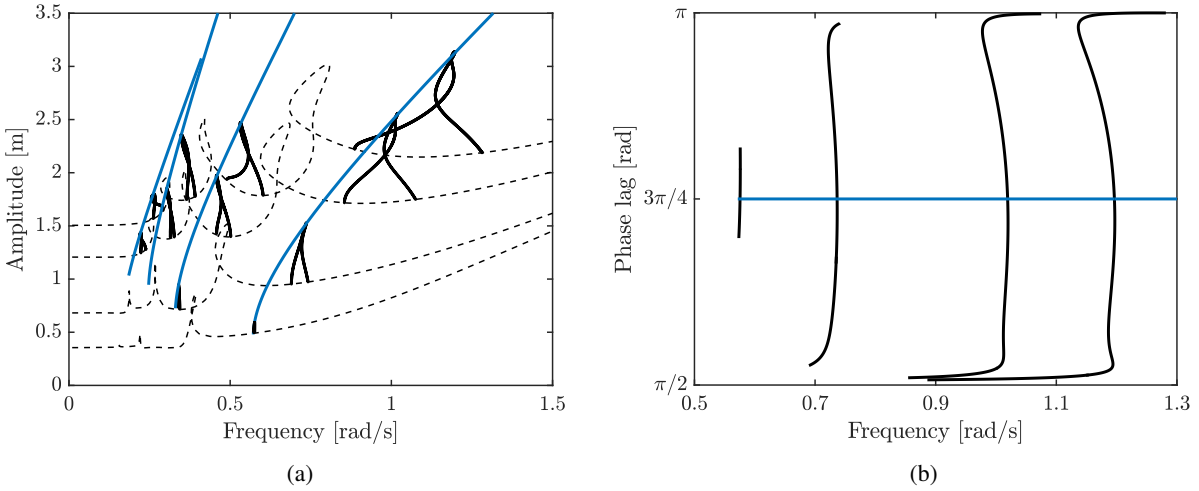


Figure 16: NFRCs and PRNMs of the even superharmonic resonances for 4 forcing amplitudes: (a) amplitude and (b) phase lag of the 2nd harmonic component for the 2:1 superharmonic resonance. Black: NFRC; blue: PRNM.

3.3.3 Subharmonic resonances

The PRNMs of the 1:3 and 1:2 subharmonic resonances are represented in Figure 17, where the phase lags at resonance are $\pi/2$ and $3\pi/8$, respectively. An important remark is that a critical forcing amplitude is required to activate the resonances. Below this forcing, the isolated resonance branch, and, hence, the PRNM, do not exist.

3.3.4 Additional superharmonic and subharmonic resonances

The PRNMs of the remaining superharmonic and subharmonic resonances are displayed in Figure 18. Again, the locus of the different resonance peaks is very well captured by the PRNMs.

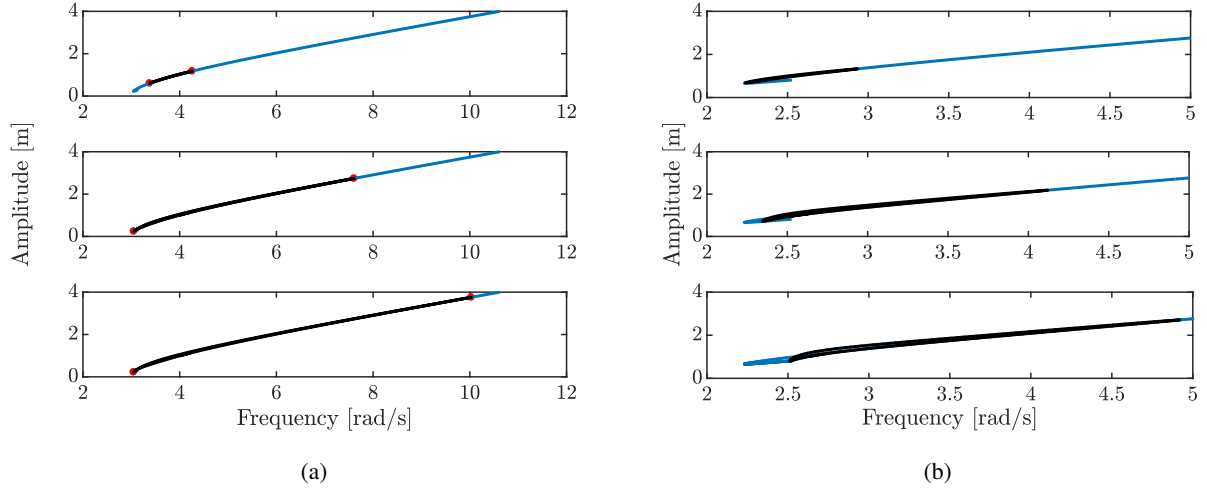


Figure 17: NFRCs and PRNMs of the 1:3 and 1:2 subharmonic resonances for 3 forcing amplitudes: (a) 1:3 and (b) 1:2. Black: NFRC; blue: PRNM.

4 PRNMs of a two-degree-of-freedom system

To establish that the PRNM definition extends well beyond the single-degree-of-freedom Duffing oscillator, a two-degree-of-freedom system with a cubic spring attached to the first mass is considered:

$$\begin{cases} \ddot{x}_1 + 0.02\dot{x}_1 - 0.01\dot{x}_2 + 2x_1 - x_2 + x_1^3 = f \sin \omega t \\ \ddot{x}_2 + 0.11\dot{x}_2 - 0.01\dot{x}_1 + 2x_2 - x_1 = 0 \end{cases} \quad (15)$$

The NFRCs for different forcing amplitudes are displayed in Figure 19. As for the Duffing oscillator, the system features superharmonic resonances depicted in Figure 19b. Specifically, 3:1 and 5:1 superharmonic resonances exist for each of the two resonances of the system. In addition, a 1:1 isolated resonance branch related to the second mode can be observed in Figure 19a for a forcing $f = 0.161\text{N}$. We note that, as for the Duffing oscillator, many other resonances exist in the system but are not further discussed herein. The PRNMs are calculated by introducing the velocity feedback at the first degree of freedom. The resulting PRNM backbones are superposed in Figure 19; they are found to offer a very accurate characterization of the resonance of both vibration modes, including the isolated resonance branch for the second mode. Besides, the four superharmonic resonance branches are also well captured by the PRNMs.

Another insightful graphical depiction exploits the fact that the introduced velocity feedback plays the role of fictitious forcing. It is therefore possible to plot the evolution of the amplitude and frequency of the PRNMs with respect to the external forcing, as achieved in Figures 20b and 20c, respectively. Interestingly, for $f = 0.161\text{N}$ in Figure 20b, three resonance points exist for the second mode (see the red dots). The point with the lowest amplitude corresponds to the usual resonance peak whereas the other two points are associated with the extremities of the isolated resonance. Thus, such a plot nicely reveals the existence of the isolated resonance. The frequencies associated with the isolated branch can be read in Figure 20c.

5 Conclusion

The concept of phase resonance/phase quadrature is well-known in linear systems theory and begins to be exploited for the experimental characterization of the fundamental resonances of nonlinear mechanical systems. The objective of this paper was to carry out a detailed study of the phase lags associated with superharmonic and subharmonic resonances of the Duffing oscillator. The study has revealed that phase quadrature still holds for $k : \nu$ resonances when k and ν are both odd. Otherwise, resonance occurs for a phase lag equal to $3\pi/4\nu$.

To provide a 1:1 correspondence between nonlinear modes and resonances, a new definition of a NNM, termed PRNM, was introduced herein. The PRNMs of the $k : \nu$ resonance correspond to the periodic responses obtained by feeding back the delayed velocity of the harmonic component k/ν into the autonomous system at the point where the external forcing is located. An efficient computational method of the PRNMs based on the HBM was also devised.

Compared to the existing NNM definitions which necessarily imply multi-point, multi-harmonic forcing, the PRNMs can be identified experimentally using single-point, single-harmonic forcing. In addition, unlike the other definitions, there is the guarantee that the PRNMs are actual solutions on the NFRC, which eliminates the lack of significance and of predictive capability of NNMs pointed out in previous studies [11, 12].

Future work will consider a more thorough study of multi-degree-of-freedom systems with a close look at modal interactions. The experimental identification of PRNMs will also be attempted. Because the identification process will involve direct velocity feedback, it should not require any precise tuning of the excitation, which, we anticipate, will be another important advantage of the PRNM definition.

References

- [1] D. J Ewins. *Modal testing : theory, practice, and application*. Baldock, Hertfordshire, England ; Philadelphia, PA : Research Studies Press, 2nd edition, 2000.
- [2] Gaëtan Kerschen, Keith Worden, Alexander F. Vakakis, and Jean-Claude Golinval. Past, present and future of nonlinear system identification in structural dynamics. *Mechanical Systems and Signal Processing*, 20(3):505 – 592, 2006.
- [3] A.F. Vakakis, L.I. Manevitch, Y.V. Mikhlin, V.N. Pilipchuk, and A.A. Zevin. *Normal Modes and Localization in Nonlinear Systems*. John Wiley & Sons, New York, 1996.
- [4] R. M. Rosenberg. Normal modes of nonlinear dual-mode systems. *Journal of Applied Mechanics*, 27(2):263–268, 1960.
- [5] R. M. Rosenberg. The Normal Modes of Nonlinear n-Degree-of-Freedom Systems. *Journal of Applied Mechanics*, 29(1):7–14, 03 1962.
- [6] G. Kerschen, M. Peeters, J.C. Golinval, and A.F. Vakakis. Nonlinear normal modes, part i: A useful framework for the structural dynamicist. *Mechanical Systems and Signal Processing*, 23(1):170 – 194, 2009.
- [7] Malte Krack. Nonlinear modal analysis of nonconservative systems: Extension of the periodic motion concept. *Computers & Structures*, 154:59 – 71, 2015.
- [8] Steven Shaw and Christophe Pierre. Non-linear normal modes and invariant manifolds. *Journal of Sound and Vibration*, 150(1):170–173, 1991.
- [9] S.W. Shaw and C. Pierre. Normal modes for non-linear vibratory systems. *Journal of Sound and Vibration*, 164(1):85 – 124, 1993.
- [10] George Haller and Sten Ponsioen. Nonlinear normal modes and spectral submanifolds: Existence, uniqueness and use in model reduction. *Nonlinear Dynamics*, 86(3):1493–1534, 2016.
- [11] Mattia Cenedese and G. Haller. How do conservative backbone curves perturb into forced responses ? a melnikov function analysis. *Proceedings of the Royal Society A: Mathematical, Physical and Engineering Sciences*, 476, 2020.
- [12] TL Hill, A Cammarano, SA Neild, and DAW Barton. Identifying the significance of nonlinear normal modes. *Proceedings. Mathematical, physical, and engineering sciences*, 473(2199), March 2017.
- [13] M. Peeters, G. Kerschen, and J.C. Golinval. Dynamic testing of nonlinear vibrating structures using nonlinear normal modes. *Journal of Sound and Vibration*, 330:486–509, 2011.
- [14] Alexander F. Vakakis and Antoine Blanchard. Exact steady states of the periodically forced and damped duffing oscillator. *Journal of Sound and Vibration*, 413:57 – 65, 2018.
- [15] T.L. Hill, A. Cammarano, S.A. Neild, and D.J. Wagg. Interpreting the forced responses of a two-degree-of-freedom nonlinear oscillator using backbone curves. *Journal of Sound and Vibration*, 349:276 – 288, 2015.
- [16] M. Peeters, G. Kerschen, and J.C. Golinval. Modal testing of nonlinear vibrating structures based on nonlinear normal modes: Experimental demonstration. *Mechanical Systems and Signal Processing*, 25(4):1227 – 1247, 2011.
- [17] L. Renson, A. Gonzalez-Buelga, D.A.W. Barton, and S.A. Neild. Robust identification of backbone curves using control-based continuation. *Journal of Sound and Vibration*, 367:145 – 158, 2016.
- [18] David A. Ehrhardt and Matthew S. Allen. Measurement of nonlinear normal modes using multi-harmonic stepped force approximation and free decay. *Mechanical Systems and Signal Processing*, 76-77:612 – 633, 2016.

- [19] Robert Szalai, David Ehrhardt, and George Haller. Nonlinear model identification and spectral submanifolds for multi-degree-of-freedom mechanical vibrations. *Proceedings of the Royal Society A: Mathematical, Physical and Engineering Sciences*, 473, 2017.
- [20] Vivien Denis, M Jossic, C. Giraud-Audinec, B. Chomette, and Olivier Thomas. Identification of nonlinear modes using phase-locked-loop experimental continuation and normal form. *Mechanical Systems and Signal Processing*, 106, 2018.
- [21] M. Scheel, S. Peter, R. Leine, and M. Krack. A phase resonance approach for modal testing of structures with nonlinear dissipation. *Journal of Sound and Vibration*, 435, 2018.
- [22] U. Parlitz and W. Lauterborn. Superstructure in the bifurcation set of the duffing equation. *Physics Letters*, 107A:351–355, 1985.
- [23] F De Veubeke. A variational approach to pure mode excitation using characteristic phase lag theory. *Technical report*, 1956.
- [24] I. Sokolov and V. Babitsky. Phase control of self-sustained vibration. *Journal of Sound and Vibration*, 248, 2001.

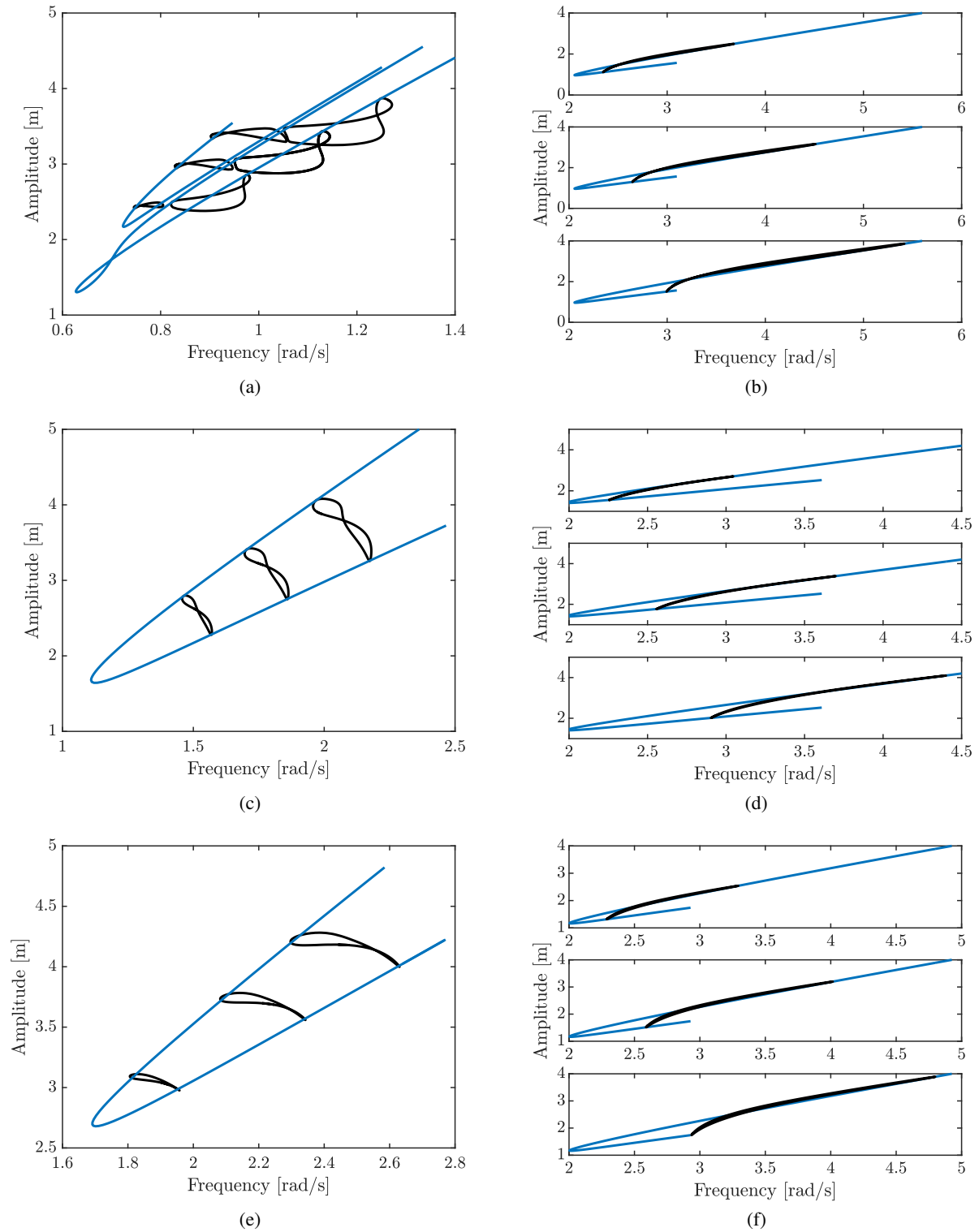


Figure 18: NFRCs and PRNMs for (a) 7:3, (b) 3:5, (c) 3:2, (d) 3:4, (e) 4:3 and (f) 2:3. Black: NFRC; blue: PRNM.

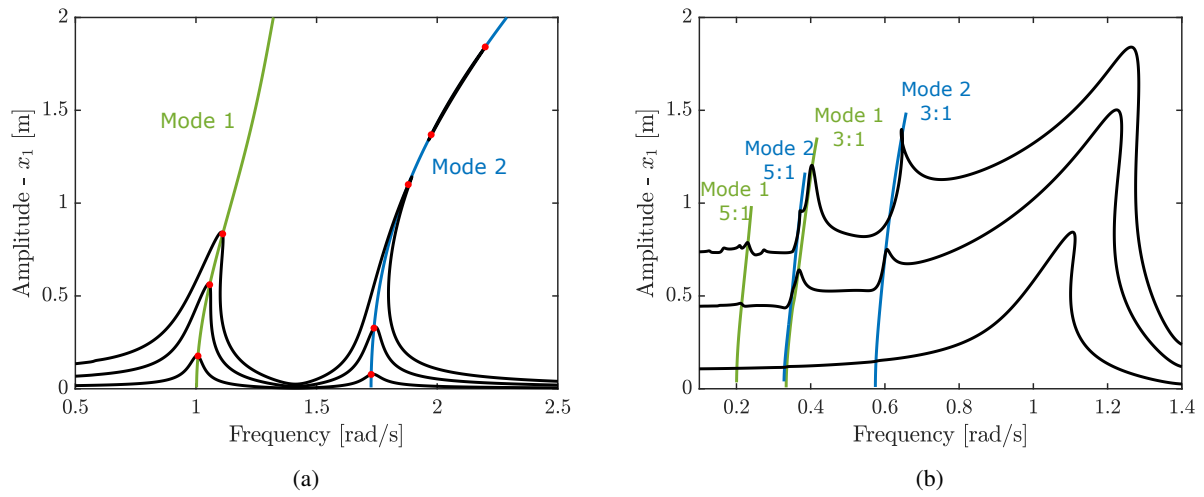


Figure 19: NFRCS and PRNMs for the 2DOF system: (a) The two vibration modes ($f = 0.02$ to $0.161N$) and (b) close-up around the superharmonic resonances ($f = 0.161$ to $1.5N$). Black: NFRCS; green: PRNMs of mode 1; blue: PRNMs of mode 2.

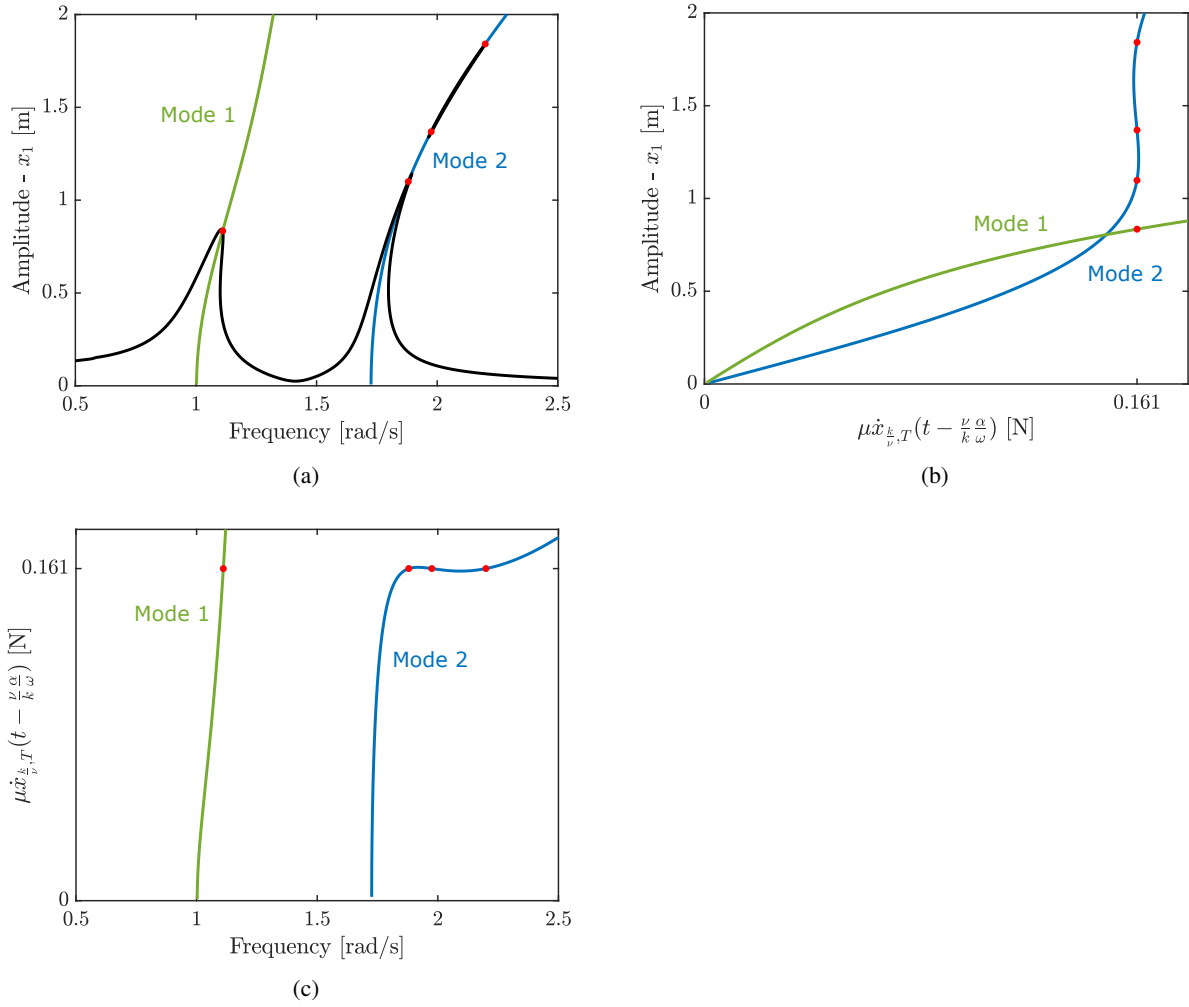


Figure 20: PRNMs for the 2DOF system: (a) NFRC (in black) for $f = 0.161N$, (b) PRNM amplitude at the first degree of freedom and (c) PRNM frequency.